

C 80-055

# Calculation of Wing-Body Pressures in Incompressible Flow Using Green's Function Method

Shinji Suzuki\* and Kyuichiro Washizu†  
University of Tokyo, Tokyo, Japan

In the present paper, the finite element technique is applied to the calculation of three-dimensional steady incompressible potential flow around a wing-body combination, the main emphasis being placed upon the study of the aerodynamic interference effect between the wing and the body. The formulation of the problem is made in the form of an integral equation following Morino's method. By the use of the finite element technique combined with the collocation method, this integral equation is reduced to a set of linear algebraic equations. By solving this set, the pressure distribution over the surface of the wing-body combination is obtained. Wind tunnel experiments have been conducted at National Aerospace Laboratory of Japan in pace with the numerical analysis. It has been found that agreement between the numerical results obtained by the present method and those obtained by the wind tunnel experiments is very encouraging.

## Introduction

**A**N important and challenging aerodynamic problem for the aerospace engineer is the evaluation of the pressure distribution on the surface of a flight vehicle, not only from the viewpoint of performance, but also of aeroelasticity, stability, and control. Extensive investigations have been and are being conducted involving numerical analysis of the problem as described in Refs. 1-9, for example. However, the flight vehicle has a complicated configuration in general, and numerical analysis requires tremendous computation labor and time. Consequently there has been a strong demand for the aerospace engineer, who is currently struggling with the rapid development of computer-aided design (CAD), to establish a computation procedure which can solve this kind of problem numerically with good accuracy and in reasonable computing time.

In the present paper, we consider the flow around a streamlined wing-body combination, which frequently will be called an airplane hereafter for the sake of simplicity, and put main emphasis on the aerodynamic interference effect between wing and body. We confine our interest to steady and incompressible flow, and assume the wing-body combination to be stationary. We also assume the flow to be inviscid and irrotational, remembering that the flow around a streamlined flight vehicle can be assumed to be potential for many practical cases.

In the present paper, Morino's method<sup>10-12</sup> is used for formulating the problem in the form of an integral equation. By the use of the finite element technique combined with the collocation method, which is sometimes called a panel method, this integral equation is reduced to a set of linear algebraic equations. By solving the set, we obtain values of the disturbance velocity potential on each element, which are

then used for numerically calculating the pressure distribution over the surface of the wing-body combination.

The present paper has three distinguishing characteristics:

1) A method is proposed for numerical calculation of the pressure acting over the airplane surface, by the use of values of the velocity potential  $\Phi$  at the centroids of four adjacent quadrilateral elements, as explained later in the section entitled "Discretization."

2) Wind tunnel experiments have been conducted along with the authors' numerical analysis, by T. Ichikawa and M. Yanagizawa and their laboratory staff at the National Aerospace Laboratory of Japan for checking the validity of the present numerical method. It has been found that agreement between the numerical results obtained by the present method and those by the wind tunnel experiments is very encouraging.

3) The computing technique proposed here has been found to give desired results with good accuracy and with reasonable computing time, and to suggest that it can be used for practical design purposes.

## Formulation of the Problem

We consider a wing-body combination placed in a uniform flow  $U_\infty$  as shown in Fig. 1. Assuming the flow around the wing-body combination to be steady, incompressible, inviscid, and irrotational, we have the governing equation for the flow as

$$\frac{\partial^2 \varphi}{\partial x^2} + \frac{\partial^2 \varphi}{\partial y^2} + \frac{\partial^2 \varphi}{\partial z^2} = 0 \quad (1)$$

while the boundary condition is given by

$$\frac{\partial \varphi}{\partial n} = -U_\infty \cdot n \quad \text{on } S_A \quad (2)$$

where  $\varphi$  is the disturbance velocity potential which is related to the velocity potential  $\Phi(x, y, z)$  and the velocity  $v(x, y, z)$  of the flow by the following relations:

$$v = \text{grad} \Phi = U_\infty + \text{grad} \varphi \quad (3)$$

In Eq. (2),  $S_A$  is the surface of the airplane, and  $n$  is unit normal drawn on  $S_A$  into the interior of the flow. The

Received Aug. 30, 1979; revision received Dec. 7, 1979. Copyright © American Institute of Aeronautics and Astronautics, Inc., 1979. All rights reserved. Reprints of this article may be ordered from AIAA Special Publications, 1290 Avenue of the Americas, New York, N.Y. 10019. Order by Article No. at top of page. Member price \$2.00 each, nonmember, \$3.00 each. Remittance must accompany order.

Index categories: Aerodynamics; Computational Methods; Subsonic Flow.

\*Graduate Student, Department of Aeronautics.

†Professor of Aeronautics and Astronautics, Department of Aeronautics. Member AIAA.

00001  
20005  
20016

Next, we take the  $a_1$  axis in the direction of  $\lambda_1$ , and the  $a_2$  axis in the direction perpendicular to  $\lambda_1$  in the plane spanned by  $\lambda_1$  and  $\lambda_2$ . Denoting the unit vectors in the directions of the

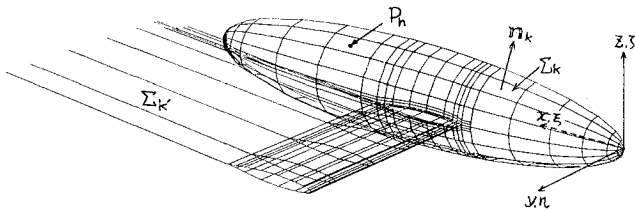
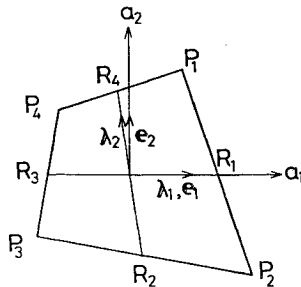


Fig. 2 Mesh division of mid-wing airplane.

Fig. 3 Local coordinate used in calculation of  $C_p$ .

$a_1$  and  $a_2$  axes by  $e_1$  and  $e_2$ , respectively, we have

$$\Phi_{a_1} = \frac{\partial \Phi}{\partial a_1} = \frac{d\Phi}{d\lambda_1} \quad (10a)$$

$$\Phi_{a_2} = \frac{\partial \Phi}{\partial a_2} = \left\{ \frac{d\Phi}{d\lambda_2} - (\lambda_2 \cdot e_1) \frac{d\Phi}{d\lambda_1} \right\} / (\lambda_2 \cdot e_2) \quad (10b)$$

By the use of these relations, we obtain the velocity and the nondimensionalized pressure at the intersection point of the  $a_1$  and  $a_2$  axes as follows

$$(\Phi_{a_1}^2 + \Phi_{a_2}^2)^{1/2} \quad (11)$$

and

$$C_p = 1 - (\Phi_{a_1}^2 + \Phi_{a_2}^2) / U_\infty^2 \quad (12)$$

As mentioned above, we have assumed a constant singularity distribution in each element. It is noted here that the constant singularity formulation is accurate only when the surface velocities are computed by differentiating the velocity potential given at the element control points. The off-body velocities near the configuration are not accurate since they are computed by summation of velocity influence coefficients and this limits the general applicability of the approach based upon the constant singularity distribution.

### Mid-Wing Airplane

First, the mid-wing airplane shown in Fig. 1 is treated. We choose the shape of the body to be an ellipsoid of revolution. We take the  $x$  axis in coincidence with the axis of revolution of the body, the  $y$  axis in the starboard direction, and the  $z$  axis in the upward direction, while the origin of the coordinate system is taken at the nose of the body. For defining the coordinates of the surface of the body, two parameters  $x$  and  $\theta$  are employed, where  $\theta$  is the angle measured from the bottom of the body as shown in Fig. 1. A curve on the surface of the body, along which  $\theta$  is constant, will be called a meridian.

The wing is assumed to have a rectangular planform, symmetrical airfoil section, no twist, and no dihedral. It is attached to the body with zero incidence angle at  $\pm 90$  deg meridian positions as shown in Fig. 1. The flow velocity  $U_\infty$  is assumed to be in the  $(x, z)$  plane and the angle of attack  $\alpha$  is

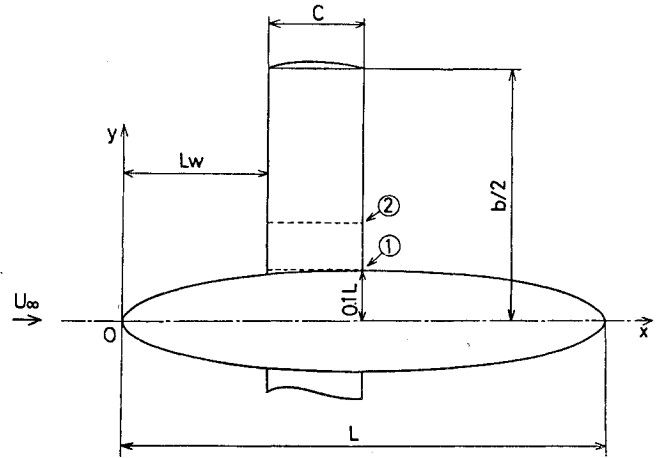


Fig. 4 Plan view of mid-wing airplane.

assumed small. Since the symmetry of the flowfield has been thus assured, only half of the flowfield is to be analyzed.

For the analysis of the mid-wing airplane, we shall employ the following two assumptions:

1) On the location of  $C_w$  on the rear part of the body: The curve  $C_w$  on the rear part of the body is assumed to be in coincidence with  $\pm 90$  deg meridian curves and continuous with the trailing edges of the wing.

2) On the shape of  $S_w$ : The wake surface  $S_w$  is assumed to consist of a family of semi-infinite straight lines which start from  $C_w$  and extend to infinity in the direction parallel to the uniform flow  $U_\infty$ .

Obviously, the flow separation occurs somewhere in the tail part of the body and the spread of the separated region depends upon the angle of attack. However, we employed the first assumption taking experimental evidence, which will be explained later, into account and remembering that the wake surface  $S_w$  has been assumed to be a sheet of zero thickness. The second assumption may be removed if the shape of  $S_w$  is determined by an iterative method such as that mentioned in Ref. 13, for example. However, the second assumption is employed in our formulation because of its simplicity, and also because the use of the second assumption will probably not deteriorate the accuracy of the numerical results significantly as far as the pressure distribution over  $S_A$  is concerned.

By the use of the above method, the pressure distribution has been calculated for a mid-wing airplane, of which the plan view is shown in Fig. 4. The wing is of a rectangular planform having aspect ratio of 5, namely  $b/c=5$ , where  $b$  and  $c$  are the span and the chord of the wing, respectively, while the body is an ellipsoid of revolution having fineness ratio of 5. The span of the wing is taken equal to the length of the fuselage denoted by  $L$ , namely,  $b=L$ . The wing has NACA 65A010 section and is fixed to the body with zero incidence angle at  $L_w=0.3L$  and  $\theta=90$  deg, where  $L_w$  is the position of the leading edge of the wing. Two spanwise stations,  $y/c=0.513$  and  $1.025$ , denoted by ① and ②, respectively, are shown in the same figure for later reference.

Mesh division is made as shown in Fig. 2. Due to the symmetry property of the present problem, only the starboard half was treated, dividing the wing surface into 126 elements and the body surface into 238 elements, while  $S_w$  in the rear parts of the wing and the body is divided into 7 and 8 strip elements, respectively.

Figure 5 shows pressure distributions over the wing surface at two spanwise stations,  $y/c=0.513$  and  $1.025$  for  $\alpha=3.74$  deg. In the figure, the abscissa is the nondimensionalized chordwise coordinate  $x/c$ , where  $x/c=0$  and  $1.0$  correspond to the leading and trailing edges, respectively, while the ordinate is the nondimensionalized pressure  $C_p$  defined by Eq.

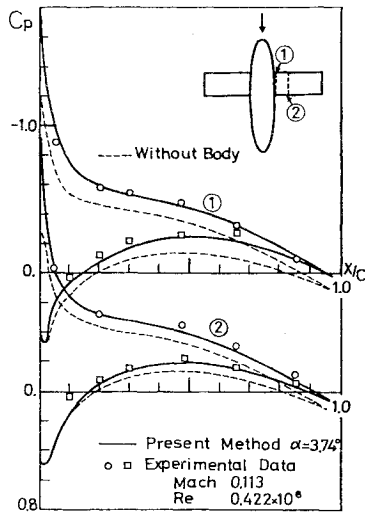


Fig. 5 Chordwise pressure distributions acting on wing surface at  $\alpha = 3.74$  deg.

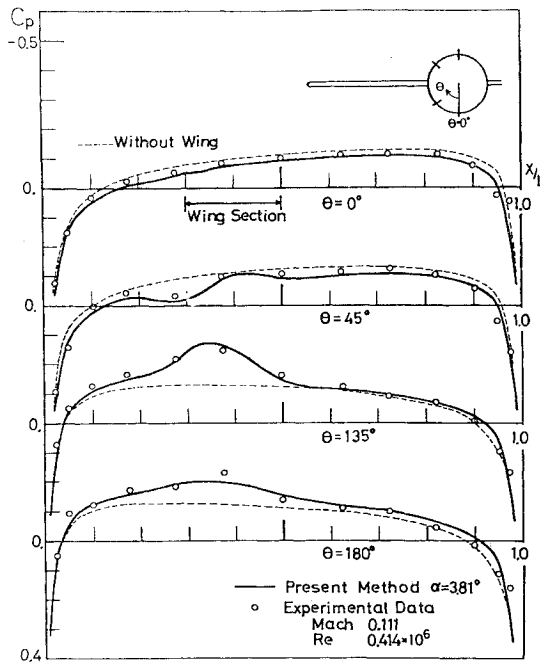


Fig. 6 Pressure distributions acting on body surface at  $\alpha = 3.81$  deg.

(4). Figure 6 shows pressure distributions over the body surface along four meridian curves:  $\theta = 0, 45, 135$ , and  $180$  deg for  $\alpha = 3.81$  deg. In the figure, the abscissa is non-dimensionalized longitudinal coordinate  $x/L$ , where  $x/L = 0$  and  $1.0$  correspond to the nose and tail of the body, respectively, while the ordinate is  $C_p$ . "Wing section" in the figure indicates the position of the wing. In these figures, the solid lines represent results obtained by the present method, while discrete symbols,  $\circ$  and  $\square$ , represent experimental results obtained by the National Aerospace Laboratory of Japan.<sup>14</sup> It is seen that agreement between the numerical and experimental results is very good. It is noted here that the dotted lines in Fig. 5 indicate the pressure distribution over the wing without the body, namely the wing alone, while those in Fig. 6 indicate the pressure distribution over the body without the wing, namely the body alone. The effect of interference between the wing and body can be clearly observed from these figures.

The flow velocity vectors over the body surface were also calculated for  $\alpha = 3.81$  deg. On the other hand, a wind tunnel

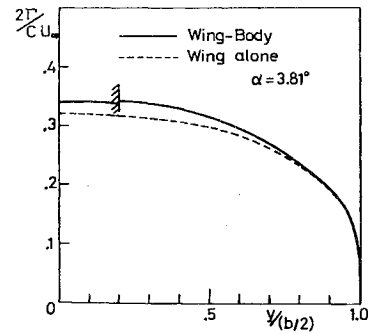


Fig. 7 Spanwise circulation distributions at  $\alpha = 3.81$  deg.

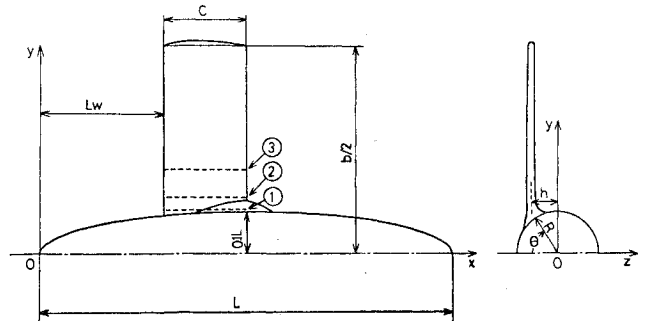


Fig. 8 Plan and front views of low-wing airplane.

experiment involving the use of tufts has been conducted by the National Aerospace Laboratory of Japan to investigate the flow characteristics over the body surface. The calculated flow velocity vectors have been found to be in good qualitative agreement with the tuft experiment, except for a small region at the tail part of the body due to the flow separation, and this seems to support our assumption about the location of  $C_w$  in the rear part of the body.

Figure 7 shows the calculated circulation distribution along the span. The abscissa is the non-dimensionalized span coordinate  $y/(b/2)$  and the ordinate is the non-dimensionalized circulation  $2\Gamma(y)/cU_\infty$  for  $\alpha = 3.81$  deg, where  $\Gamma(y)$  is the circulation at the spanwise station  $y$  and is obtainable by the use of Eq. (5) as follows:

$$\Gamma(y) = \varphi_+(y) - \varphi_-(y) \quad (13)$$

In this figure, the solid and dotted curves indicate the circulation distribution over the wing-body combination and the wing alone, respectively. This figure indicates that the lift has increased by the presence of the body and that the lift acting on the body is of the same order of magnitude as that acting on the corresponding part of the wing alone. It seems that the present assumption about the location of  $C_w$  over the rear part of the body should be improved from the viewpoint of the circulation distribution.

It is finally noted that the computation has been carried out by HITAC 8700/8800 of the University of Tokyo, and computing time for obtaining Figs. 5 and 6 was 190 s.

### Low-Wing Airplane

Next, we proceed to investigate the flowfield around a low-wing airplane as shown in Fig. 8. The wing is of rectangular planform having aspect ratio of 5, NACA 65A010 section, no twist, and no dihedral, while the body is an ellipsoid of revolution having fineness ratio of 5. The span of the wing is taken to be equal to the length of the body. The wing is fixed to the body with zero incidence angle at  $L_w = 0.3L$  and  $h/R = 2/3$  as shown in Fig. 8, where  $h$  is the distance between the  $x$  axis and the middle plane of the wing, while  $R$  is the

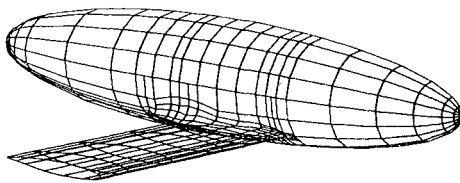
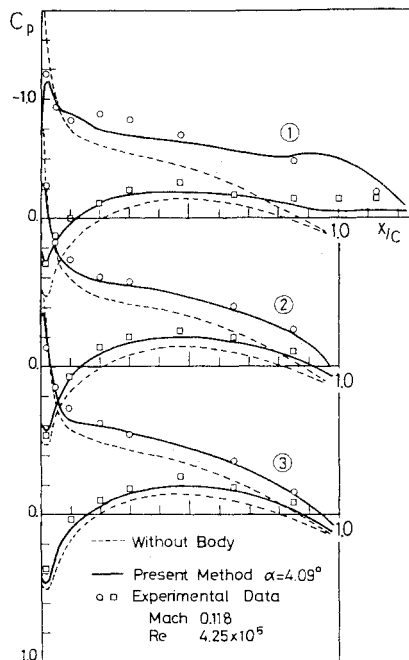


Fig. 9 Mesh division of low-wing airplane.

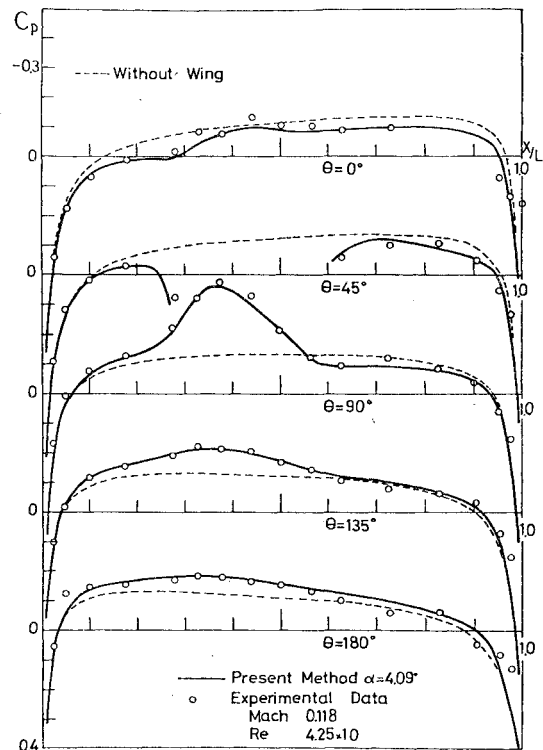
Fig. 10 Chordwise pressure distributions acting on wing at  $\alpha = 4.09$  deg.

maximum radius of the body. A fillet is attached on both sides of the wing between the wing and the body to avoid premature separation due to the interference between the wing and the body. Three spanwise stations,  $y/c = 0.513, 0.688$ , and  $1.025$ , denoted by ①, ②, and ③, respectively, are shown in the same figure for later reference.

For the analysis of the low-wing airplane, we shall assume the location of  $C_w$  over the rear part of the body in such a way that it coincides with the meridian curves which are continuous with the trailing edges of the fillets, namely  $\theta = \pm \cos^{-1}(h/R)$  meridians. As will be explained later, this assumption has been found to provide results which are in good agreement with our experiments. The wake surface  $S_w$  is assumed to consist of a family of semi-infinite straight lines which start from  $C_w$  and extend to infinity in the direction parallel to the uniform velocity  $U_\infty$ .

Mesh division is as shown in Fig. 9. Due to the symmetry property of the present problem, only the starboard half was treated: the surface of the airplane  $S_A$  and the wake surface  $S_w$  are divided into 373 quadrilateral elements and 15 strip elements, respectively.

Figure 10 shows the pressure distributions over the wing surface at three spanwise stations,  $y/c = 0.513, 0.688$ , and  $1.025$  for  $\alpha = 4.09$  deg. In the figure, the abscissa is the nondimensionalized chordwise coordinate, while the ordinate is the nondimensionalized pressure. Figure 11 shows the pressure distributions over the body surface along five meridian curves,  $\theta = 0, 45, 90, 135$ , and  $180$  deg for  $\alpha = 4.09$  deg. In the figure, the abscissa is the nondimensionalized longitudinal coordinate, while the ordinate is the nondimensionalized pressure. In these figures, the solid lines

Fig. 11 Pressure distributions acting on body surface at  $\alpha = 4.09$  deg.

represent results obtained by the present method, while discrete symbols,  $\circ$  and  $\square$ , represent experimental results obtained by the National Aerospace Laboratory of Japan.<sup>15</sup> It is noted that the dotted lines in Fig. 10 indicate the pressure distributions over the wing without the body, namely the wing alone, while those in Fig. 11 indicate the pressure distributions over the body without the wing, namely the body alone.

It is seen in Figs. 10 and 11 that agreement between numerical and experimental results is encouraging, and that the effect of interference among the wing, the body, and the fillet have been clearly indicated. It is added that numerical analysis has been carried out for several angles of attack and the pressure distributions obtained by the present numerical method have been found to be in good agreement with those obtained experimentally for the range of angle of attack,  $-4$  deg  $\leq \alpha \leq +8$  deg.

The flow velocity vectors over the body surface were also calculated, and compared with a wind tunnel experiment in which white paste was painted on the body surface to investigate the flow directions over it.<sup>15,16</sup> It has been found that the calculated flow velocity vectors are in good qualitative agreement with the experiments, except for a small region at the tail part of the body due to the flow separation, and this seems to support our assumption on the location of  $C_w$  in the rear part of the body. Needless to say, however, further study should be carried out to find a better and more reasonable mathematical modelling of the flowfield around the body and its wake to broaden the applicability of the present method.

It is noted that the computation was carried out by HITAC 8700/8800 of the University of Tokyo and computing time for obtaining Figs. 10 and 11 was about 200 s.

It is finally noted that the present method has been applied to several other examples, including a T-wing, an inverted T-wing, a rectangular wing with two rectangular end plates, and a cruciform wing with and without a fillet.<sup>16-19</sup> The agreement between numerical and experimental results have been found to be very good. These seem to have enhanced the practical value of the present finite element technique.

### Conclusion

It has been shown that the finite element technique presented in the present paper provides an effective tool for numerical analysis of steady incompressible flow about a three-dimensional streamlined body such as an airplane. Numerical computations have been carried out and results have been obtained with good accuracy and in reasonable computing time, suggesting that the present technique can be used for practical design purposes.

As mentioned in the Introduction, the present paper put main emphasis on the study of the interference effect between the wing and the body. However, the present technique would provide a practical numerical method for obtaining aerodynamic characteristics such as aerodynamic derivatives of the airplane, if further work would be carried out to find a better and more reasonable mathematical modelling of the flowfield around the airplane.

### Acknowledgment

The authors would like to express their sincere appreciation to T. Ichikawa and his staff, and to M. Yanagizawa and his staff of the National Aerospace Laboratory of Japan, who collaborated with the authors in conducting the wind tunnel experiments in pace with the authors' numerical work. Without their collaboration, the present paper would not have been realized. The authors wish also to express their gratitude to the referees for valuable comments.

### References

- <sup>1</sup>Ashley, H. and Roden, W.P., "Wing-Body Interaction," *Annual Review of Fluid Mechanics*, Vol. 4, Annual Reviews, Inc., Palo Alto, Calif., 1972, pp. 431-472.
- <sup>2</sup>Thomas, J.L., "Subsonic Finite Elements for Wing-Body Combinations. Vortex-Lattice Utilization," NASA SP-405, May 1976, pp. 11-26.
- <sup>3</sup>Rubbert, P.E. and Saaris, G.R., "Review and Evaluation of a Three Dimensional Lifting Potential Flow Analysis Method for Arbitrary Configurations," AIAA Paper 72-188, 1972.
- <sup>4</sup>Bisplinghoff, R.L. and Ashley, H., *Principle of Aeroelasticity*, John Wiley and Sons, New York and London, 1962.
- <sup>5</sup>McDonnell Douglas Corp., USAF Stability and Control DAT-COM, 1968.
- <sup>6</sup>Woodward, F.A., "Analysis and Design of Wing-Body Combinations at Subsonic and Supersonic Speeds," *Journal of Aircraft*, Vol. 5, Nov.-Dec. 1968, pp. 528-534.
- <sup>7</sup>Labrujere, T.E., Loeve, W., and Sloof, J.W., "An Approximation Method for the Calculation of the Pressure Distribution on Wing-Body Combination at Subcritical Speeds," AGARD CP 71, 1971, pp. 11-1—11-15.
- <sup>8</sup>Giesing, J.P., Kalman, T.P., and Rodden, W.P., "Subsonic Steady and Oscillatory Aerodynamics for Multiple Interfering Wings and Bodies," *Journal of Aircraft*, Vol. 9, Oct. 1972, pp. 693-702.
- <sup>9</sup>Hess, J.L., "Calculation of Potential Flow Around Arbitrary Three Dimensional Lifting Bodies, Final Technical Report," McDonnell Douglas Report MDC J5679-01, 1972.
- <sup>10</sup>Morino, L., "A General Theory of Unsteady Compressible Potential Aerodynamics," NASA CR-2464, Dec. 1974.
- <sup>11</sup>Kuo, C.C., and Morino, L., "Steady Subsonic Flow Around Finite Thickness Wings," NASA CR-2612, Nov. 1975.
- <sup>12</sup>Morino, L., Chen, L.T., and Suciu, E.O., "Steady and Oscillatory Subsonic and Supersonic Aerodynamics around Complex Configurations," *AIAA Journal*, Vol. 13, March 1975, pp. 368-374.
- <sup>13</sup>Belotserkovskiy, S.M., "Calculation of the Flow around Wings of Arbitrary Planform in a Wide Range of Angles of Attack," NASA TT F 12291, May 1969.
- <sup>14</sup>Yanagizawa, M. and Kikuchi, K., "Study for Characteristics of Wing-Body Combination," *Proceedings of 9th Annual Meeting of Japan Society for Aeronautical and Space Sciences*, April 1978, pp. 18-19 (in Japanese).
- <sup>15</sup>Yanagizawa, M., Kikuchi, K., and Koyama, T., "Study for Characteristics of Wing-Body Combination—Second Report" *Proceedings of 10th Annual Meetings of Japan Society for Aeronautical and Space Sciences*, April 1979, pp. 150-151 (in Japanese).
- <sup>16</sup>Suzuki, S., "A Study on the Application of the Finite Element Method to Aerodynamic Problems," Master thesis, The University of Tokyo, March 1979 (in Japanese).
- <sup>17</sup>Morita, T., Ejiri, H., and Kikuchi, T., "Measurements of Pressure Distribution on Cruciform Wing," (in Japanese), National Aerospace Laboratory, TM377, 1979.
- <sup>18</sup>Washizu, K., Suzuki, S., and Nakamura, K., "An Application of the Finite Element Method to Aerodynamic Problems of Aircraft—First Report," *Journal of Japan Society for Aeronautical and Space Sciences*, July 1979, pp. 31-38 (in Japanese).
- <sup>19</sup>Washizu, K. and Suzuki, S., "An Application of the Finite Element Method to Aerodynamic Problems of Aircraft," *Collected Papers of 28th National Congress for Theoretical and Applied Mechanics*, Nov. 1978, pp. 323-324 (in Japanese).